

Iron- and erythropoietin-resistant anemia in a spontaneous breast cancer mouse model

Nuria Fabregas Bregolat,^{1,2} Maja Ruetten,³ Milene Costa da Silva,⁴ Mostafa A. Aboouf,^{1,2,5} Hyrije Ademi,^{1,2} Nadine von Büren,^{1,2} Julia Armbruster,^{1,2} Martina Stirn,⁶ Sandro Altamura,^{4,7} Oriana Marques,^{4,7} Josep M. Monné Rodriguez,⁸ Victor J. Samillan,⁹ Rashim Pal Singh,¹⁰ Ben Wielockx,¹⁰ Martina U. Muckenthaler,^{4,7,11,12} Max Gassmann^{1,13} and Markus Thiersch^{1,2,13}

¹Institute of Veterinary Physiology, Vetsuisse Faculty, University of Zurich, Zurich, Switzerland; ²Center for Clinical Studies, Vetsuisse Faculty, University of Zurich, Zurich, Switzerland; ³PathoVet AG, Pathology Diagnostic Laboratory, Tagelswangen ZH, Switzerland ⁴Department of Pediatric Oncology, Hematology and Immunology, University of Heidelberg, Heidelberg, Germany; ⁵Department of Biochemistry, Faculty of Pharmacy, Ain Shams University, Cairo, Egypt; ⁶Clinical Laboratory, Department of Clinical Diagnostics and Services, Vetsuisse Faculty, University of Zurich, Zurich, Switzerland; ⁷Molecular Medicine Partnership Unit, Heidelberg, Germany; ⁸Laboratory for Animal Model Pathology, Institute of Veterinary Pathology, Vetsuisse Faculty, University of Zurich, Zurich, Switzerland ⁹Universidad Le Cordon Bleu, School of Human Nutrition, Lima, Peru; ¹⁰Institute of Clinical Chemistry and Laboratory Medicine, Carl Gustav Carus, TU Dresden, Germany; ¹¹Translational Lung Research Center Heidelberg (TLRC), German Center for Lung Research (DZL), University of Heidelberg, Heidelberg, Germany; ¹²German Center for Cardiovascular Research, Partner Site, Heidelberg, Germany and ¹³Zurich Center for Integrative Human Physiology (ZIHP), University of Zurich, Zurich, Switzerland

Correspondence:

Markus Thiersch
markus.thiersch@uzh.ch

Received: January 24, 2022.

Accepted: March 31, 2022.

Prepublished: April 7, 2022.

<https://doi.org/10.3324/haematol.2022.280732>

©2022 Ferrata Storti Foundation

Published under a CC-BY-NC license



Abstract

Anemia of cancer (AoC) with its multifactorial etiology and complex pathology is a poor prognostic indicator for cancer patients. One of the main causes of AoC is cancer-associated inflammation that activates mechanisms, commonly observed in anemia of inflammation, whereby functional iron deficiency and iron-restricted erythropoiesis are induced by increased hepcidin levels in response to raised levels of interleukin-6. So far only a few AoC mouse models have been described, and most of them did not fully recapitulate the interplay of anemia, increased hepcidin levels and functional iron deficiency in human patients. To test if the selection and the complexity of AoC mouse models dictates the pathology or if AoC in mice *per se* develops independently of iron deficiency, we characterized AoC in Trp53^{fllox}WapCre mice that spontaneously develop breast cancer. These mice developed AoC associated with high levels of interleukin-6 and iron deficiency. However, hepcidin levels were not increased and hypoferremia coincided with anemia rather than causing it. Instead, an early shift in the commitment of common myeloid progenitors from the erythroid to the myeloid lineage resulted in increased myelopoiesis and in the excessive production of neutrophils that accumulate in necrotic tumor regions. This process could not be prevented by either iron or erythropoietin treatment. Trp53^{fllox}WapCre mice are the first mouse model in which erythropoietin-resistant anemia is described and may serve as a disease model to test therapeutic approaches for a subpopulation of human cancer patients with normal or corrected iron levels who do not respond to erythropoietin.

Introduction

Anemia of cancer (AoC) is a common comorbidity¹ and an independent poor prognostic factor in cancer patients.² One of the most frequent types of AoC is caused by inflammation associated with cancer. Among the proinflammatory cytokines, interleukin 6 (IL-6) in particular can cause anemia by different mechanisms. IL-6 can either directly suppress erythropoiesis or inhibit erythropoiesis by interfering with iron homeostasis, the latter effect being well studied in models of anemia of inflammation. During

inflammation, IL-6 induces the hepatic expression of hepcidin,³ the master regulator of iron metabolism.^{4,5} Under physiological conditions, hepcidin expression is induced by high iron levels via the BMP/HJV/SMAD pathway.^{6,7} In contrast, hepcidin is suppressed by the erythropoietin (EPO)-induced release of erythroferrone (ERFE) from red blood cell precursors.⁸⁻¹⁰ Hepcidin regulates iron trafficking by binding and degrading the cellular iron exporter ferroportin (FPN1)^{11,12} to prevent duodenal iron absorption and iron release from hepatocytes and macrophages.¹³ Thereby, hepcidin can cause functional iron deficiency by reducing

serum iron levels and causing iron-restricted erythropoiesis even if tissue iron levels are normal or elevated.

AoC in humans is associated with increased hepcidin levels.^{14,15} Mouse models with AoC displayed inconsistent hepcidin expression despite inflammation, and the ablation of hepcidin did not change tissue and plasma iron levels.¹⁶ Mice with tumors overexpressing IL-6 showed increased liver hepcidin expression associated with anemia.^{17,18} However, inhibiting IL-6 prevented anemia without improving plasma iron levels,¹⁸ indicating that IL-6 may suppress erythropoiesis in a hepcidin- and iron-independent manner in mice. A proportion (10-30%) of human cancer patients also do not respond to combination therapies with iron and erythropoiesis-stimulating agents (ESA),¹⁹ indicating that a subpopulation of cancer patients may be resistant to ESA. Such resistance is better described in anemic patients with kidney damage, in whom chronic inflammation and pro-inflammatory cytokines can directly suppress erythropoiesis.²⁰ For example, IL-6 and interleukin-1 suppress erythropoiesis by inhibiting downstream signaling of the EPO receptor (EPOR) in erythroid precursors,^{20,21} for example, through activation of the suppressor of cytokine signaling-3 (SOCS-3).²² Interferon gamma (INF γ) and tumor necrosis factor alpha (TNF α) induce apoptosis of erythroid precursors²³ or reduce their life span.²⁴ Granulocyte colony-stimulating factor (G-CSF) and granulocyte-macrophage colony-stimulating factor (GM-CSF) also inhibit erythropoiesis in mice with AoC by interfering with red blood cell production, rather than by increasing hepcidin levels and dysregulating iron homeostasis.^{25,26}

However, the chosen model may determine the AoC pathology in mice. Because most mouse models analyzed so far were established by cancer cell injection, we characterized AoC in Trp53^{fllox}WapCre mice carrying a breast tissue-specific ablation of tumor suppressor p53 that gives rise to spontaneously occurring mammary carcinomas. In this study we investigated whether: (i) Trp53^{fllox}WapCre mice develop AoC due to functional iron deficiency or due to direct inhibition of erythropoiesis; and (ii) Trp53^{fllox}WapCre mice mirror human pathology thereby representing an adequate model to study AoC mechanisms and treatment options.

Methods

Animals

Mouse experiments were performed in accordance with the Swiss animal law and with the approval of the ethical committee (license 128/2012 and 100/2018) of the local veterinary authorities. Trp53^{fllox}WapCre mice on a clean FVB background, obtained from Thomas Rüllicke (University of Veterinary Medicine, Vienna, Austria), express Cre under

the murine whey acid promotor (WAP) to delete p53 specifically in mammary tissue giving rise to spontaneous breast tumors (Table 1). Housing conditions and tumor size measurements are described in the *Online Supplementary Information*. Mice were euthanized by CO₂ at the indicated time points or when either one single tumor reached a size of 2 cm³ or multiple tumors reached a total volume of 3 cm³. We defined this time point as terminal stage (TS). As controls we used age-matched tumor-free female Trp53^{fllox}WapCre mice (TF), i.e., mice that had not developed tumors at that point. Tissue sampling is further described in the *Online Supplementary Data*.

Additional methods

Methods describing hematology, plasma cytokine measurements, treatment with EPO and iron, and quantitative polymerase chain reaction (qPCR) analyses including the list of primers (*Online Supplementary Table S1*) are described in the *Online Supplementary Information*. Statistical and flow cytometry analyses are also described there, including antibody cocktails for hematopoiesis (*Online Supplementary Table S2*), lineage-positive cell blocking (*Online Supplementary Table S3*) and erythroid maturation (*Online Supplementary Table S4*) as well as gating strategies for hematopoietic (*Online Supplementary Figure S1A*) and late-stage erythroid cells (*Online Supplementary Figure S1B*).^{27,28}

Results

Female Trp53^{fllox}WapCre mice developed subcutaneous mammary tumors between 20 and 36 weeks of age and reached TS, as defined in the Methods section, 18 to 43 days following tumor onset (Table 1). TF Trp53^{fllox}WapCre female mice served as controls.

Trp53^{fllox}WapCre mice develop breast cancer associated with anemia

Hematocrit, hemoglobin levels and number of erythrocytes dropped from a mean of 41.1%, 13.3 g/dL, and 9.8x10⁶/ μ L in TF to 35.4% ($P<0.001$), 11.0 g/dL ($P<0.001$) and 7.7x10⁶/ μ L ($P<0.001$) in TS mice. While the proportion of overall circulating reticulocytes tended to increase, the immature reticulocyte fraction increased from 51% in TF to 56.5% in TS mice ($P<0.05$), but the mature reticulocyte fraction decreased from 49% in TF to 43.5% in TS mice ($P<0.05$) (Figure 1A, *Online Supplementary Figure S2A*). The mean corpuscular hemoglobin did not differ between TF and TS mice. The mean corpuscular hemoglobin concentration decreased from 33.2 g/dL in TF to 31.3 g/dL in TS mice ($P<0.01$) and the mean corpuscular volume increased from 42.7 fL in TF to 45.2 fL in TS mice ($P<0.01$). The red cell distribution width decreased from 23.0% in TF to 22.1% in TS

Table 1. Clinical characterization of terminal stage Trp53^{fllox}WpCre mice.

| Parameter | Range | 25 th Percentile | Median | 75 th Percentile |
|---|--|-----------------------------|--------|-----------------------------|
| Tumor onset [weeks of age] | 21-36 | 25.6 | 27.0 | 30.2 |
| Time until TS* [days] | 18-43 | 21 | 24.5 | 29.25 |
| Number of tumors at TS* | 1-6 | 2.0 | 3.0 | 4.0 |
| Loss/gain of bodyweight at TS* [g] | -1(loss) – +8 (gain) | 0 | +2.0 | +4.0 |
| Loss/gain of bodyweight at TS* [g] corrected for tumor weight | -3 (loss) – +6 (gain) | -2.0 | 0 | +2.0 |
| Further characteristics | | | | |
| Type of tumors | 6 % solid carcinoma; 12.5 % adenocarcinoma, 81.5% carcinosarcoma | | | |
| Tumor location in mammary tissue | | | | |
| Cervical mammary glands | 21.1 % | | | |
| Thoracic mammary glands | 19.7 % | | | |
| Abdominal mammary glands | 44.9 % | | | |
| Inguinal mammary glands | 14.3 % | | | |
| Metastasis | not observed | | | |
| Bleeding/blood loss | not observed | | | |
| Hemolysis | not observed | | | |

*TS: terminal stage, when either one tumor reached a size of 2 cm³ or multiple tumors reached a total volume of 3 cm³.

mice ($P=0.06$) (Figure 1B, *Online Supplementary Figure S2B*). Overall, Trp53^{fllox}WapCre tumor mice developed hypochromic, macrocytic anemia.

Trp53^{fllox}WapCre mice develop anemia of cancer associated with inflammation

Liver mRNA levels of the inflammation marker serum amyloid A1 (*Saa1*) increased 100-fold ($P<0.001$) and plasma IL-6 levels increased approximately 300-fold in TS mice ($P<0.05$), suggesting ongoing inflammation (Figure 2A). The number of circulating leukocytes in TS mice was 2.2 times higher than in TF mice ($P<0.001$). While the number of lymphocytes did not change, the number of monocytes increased 9 times in TS mice ($P<0.001$). Basophils were detected in TF but not in TS mice and eosinophils did not differ between TF and TS mice. Neutrophils increased 9.5 times in TS mice ($P<0.01$) (Figure 2B, *Online Supplementary Figure S2C*) and accumulated, together with monocytes and other leukocytes, in suppuratively inflamed tumor regions, probably contributing to tumor necrosis (Figure 2C).

Trp53^{fllox}WapCre mice develop erythropoietin- and iron-resistant anemia of cancer

Trp53^{fllox}WapCre mice showed no evidence of metastasis (Table 1) or kidney, spleen, and liver damage (*Online Supplementary Table S5*). However, the sizes of liver and spleen increased 1.5 times ($P<0.001$) and 2.5 times

($P<0.001$) (Figure 3A), respectively, the former due to increased hepatocyte proliferation (*Online Supplementary Figure S3*) and the latter probably due to increased extramedullary erythropoiesis. *Epo* mRNA levels in the kidney were 2 times higher in TS than in TF mice ($P<0.05$) and mean EPO plasma levels increased from 448 pg/mL in TF mice to 1109 pg/mL in TS mice ($P=0.06$) (Figure 3B), indicating that renal EPO synthesis was increased in TS Trp53^{fllox}WapCre mice. We next tested if exogenous EPO administration protects Trp53^{fllox}WapCre mice from anemia. EPO treatment did not alter tumor progression and increased, as expected, the hematocrit in TF mice. However, EPO did not prevent most tumor-bearing Trp53^{fllox}WapCre mice from developing AoC (Figure 3C). Only two of 14 EPO-treated TS mice probably responded with increased erythropoiesis (Figure 3C, red arrows).

Given that Trp53^{fllox}WapCre mice did not respond to EPO, we determined plasma iron levels, which can be limiting for erythropoiesis especially during inflammation. The mean iron concentration in blood plasma dropped from 240.5 µg/dL in TF to 186.7 µg/dL ($P<0.01$) in TS mice, the mean transferrin saturation decreased from 66% to 34% ($P<0.001$), and plasma ferritin was reduced by 54% ($P<0.001$) (Figure 3D, *Online Supplementary Figure S4A*). Tumor sections stained for iron as well as iron measurements in tumor samples indicated that tumors were largely iron spared and that TS mice had less iron in bone marrow,

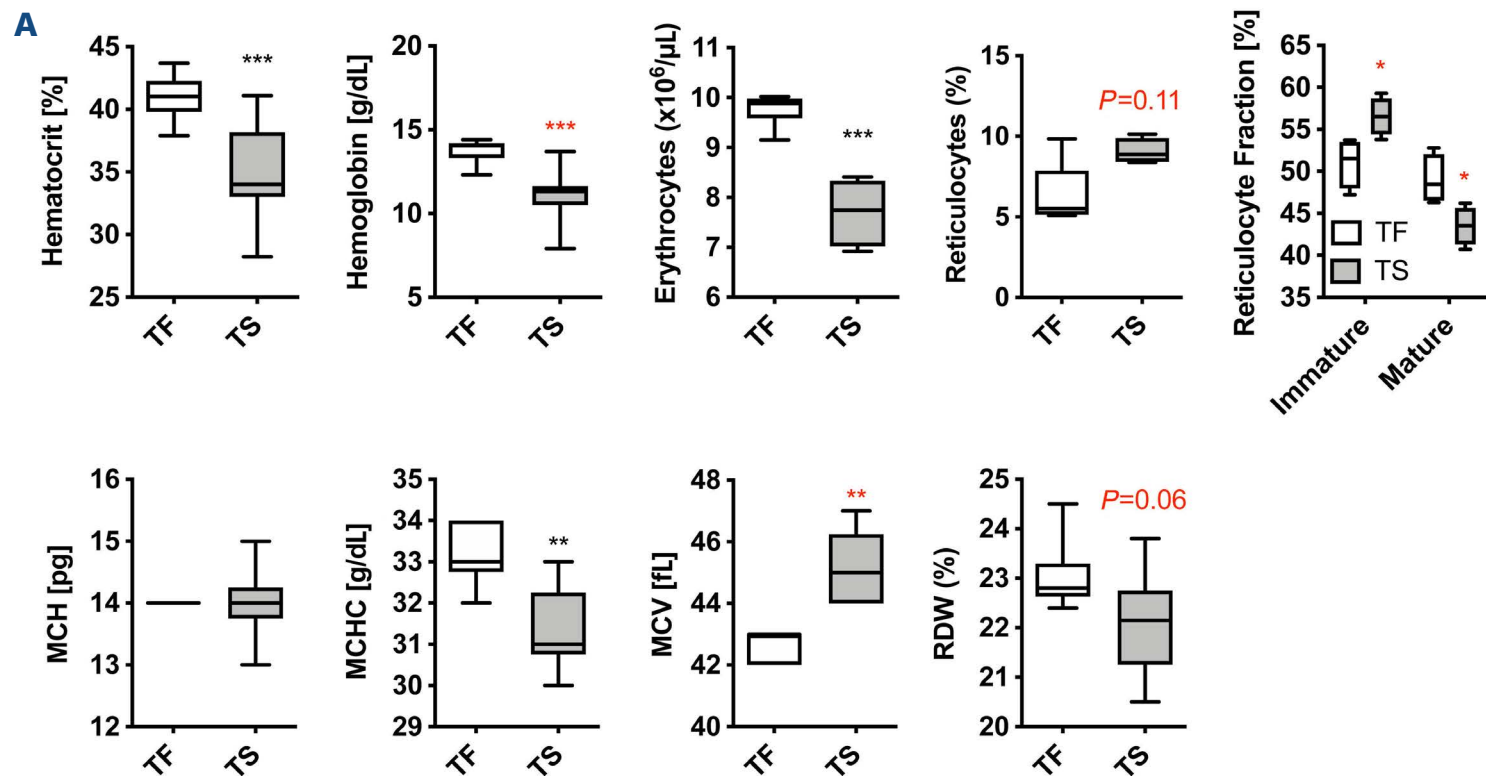


Figure 1. Anemia of cancer in *Trp53^{fllox}WapCre* breast cancer mice. Blood from tumor-bearing *Trp53^{fllox}WapCre* mice (gray boxes) was taken when the tumor reached maximal permitted size (defined as terminal stage). Age-matched tumor-free *Trp53^{fllox}WapCre* mice (white boxes) served as controls. (A) Hematocrit (n=14-15) and hemoglobin (n=16-33) analyzed by microcentrifugation and by an ABL800, respectively, as well as erythrocyte count (n=6), proportion of overall circulating reticulocytes and proportion of immature and mature reticulocyte fractions (n=4) analyzed by a Sysmex XT-2000iV from whole blood. (B) Mean corpuscular hemoglobin, mean corpuscular hemoglobin concentration, mean corpuscular volume, and red cell distribution width (n=4-6), analyzed by a Sysmex XT-2000iV from whole blood. Data are shown as a box plot with minimum to maximum whiskers and were analyzed by a Student *t*-test (black symbols) or a Mann-Whitney test (red symbols or *P*-values) (**P*<0.05, ** *P*<0.01, *** *P*<0.001). TF: tumor free; TS: terminal stage; MCH: mean corpuscular hemoglobin, MCHC: mean corpuscular hemoglobin concentration; MCV: mean corpuscular volume; RDW: red cell distribution width.

spleen, liver, and kidney than TF mice (*Online Supplementary Figure S4B, C*). Despite the high IL-6 plasma levels, plasma hepcidin did not differ between TS and TF mice. In fact, hepcidin (*Hamp1*) mRNA levels in TS mice were even 2.9 times lower (*P*<0.05) than in TF mice (Figure 3D). Hepcidin expression at earlier stages of tumor development was also not altered. Among the genes that regulate hepcidin, we observed that *Bmp6* RNA levels were reduced while *Bmp2*, *Hfe* and *Hjv* were not differentially regulated in the liver of TS mice (*Online Supplementary Figure S4D*). However, TS mice showed 1.7 times (*P*=0.07) and 5 times higher (*P*<0.05) mRNA levels of erythroferrone (*Erfe*), a suppressor of hepcidin mRNA expression, in bone marrow and spleen, respectively, compared to TF mice (Figure 3D). Notably, expression of hepcidin-suppressing platelet-derived growth factor BB (PDGF-BB) and its downstream target *Creb1*²⁹ was not altered (*Online Supplementary Figure S5*). Unchanged ferroportin (*Fpn1*) mRNA and immunohistochemically assessed FPN1 protein levels in the liver as well as increased FPN1 mRNA and protein levels in the spleen of TS mice (*Online Supplementary Figure S4E*) further indicated that hepcidin was not activated in *Trp53^{fllox}WapCre* mice. Given that commercial diets exceed the daily iron demand of mice and may therefore blunt hepcidin expression,³ we fed mice with an iron-sufficient diet. How-

ever, the diet did not alter either hepcidin expression or the extent of anemia and iron deficiency in TS mice (*Online Supplementary Figure S6*).

We concluded that TS mice developed iron deficiency and suppressed hepcidin expression through a mechanism that increases iron availability. We therefore tested if iron supplementation prevents iron deficiency and anemia in *Trp53^{fllox}WapCre* tumor mice. Given that tumor growth and time points of reaching the TS varied between 18 and 43 days among mice with tumors, we performed two iron supplementation experiments to control either the time after iron supplementation or tumor size. We injected mice intravenously with a single dose of iron or saline immediately after tumor onset and examined: (i) if anemia and iron levels changed 15 days after treatment independently of tumor size and (ii) if anemia and iron levels changed in TS mice. In both experiments, iron treatment did alter tumor proliferation, hematocrit (Figure 3E) or hemoglobin levels (*Online Supplementary Figure S7A*). While plasma iron levels were increased 15 days after iron supplementation, indicating that supplementary iron was available in the plasma at early time points, plasma iron levels in saline- or iron-treated TS mice were not altered (*Online Supplementary Figure S7B*). Accordingly, we concluded that hypoferrremia coincided with, rather than caused, AoC in *Trp53^{fllox}WapCre* mice.

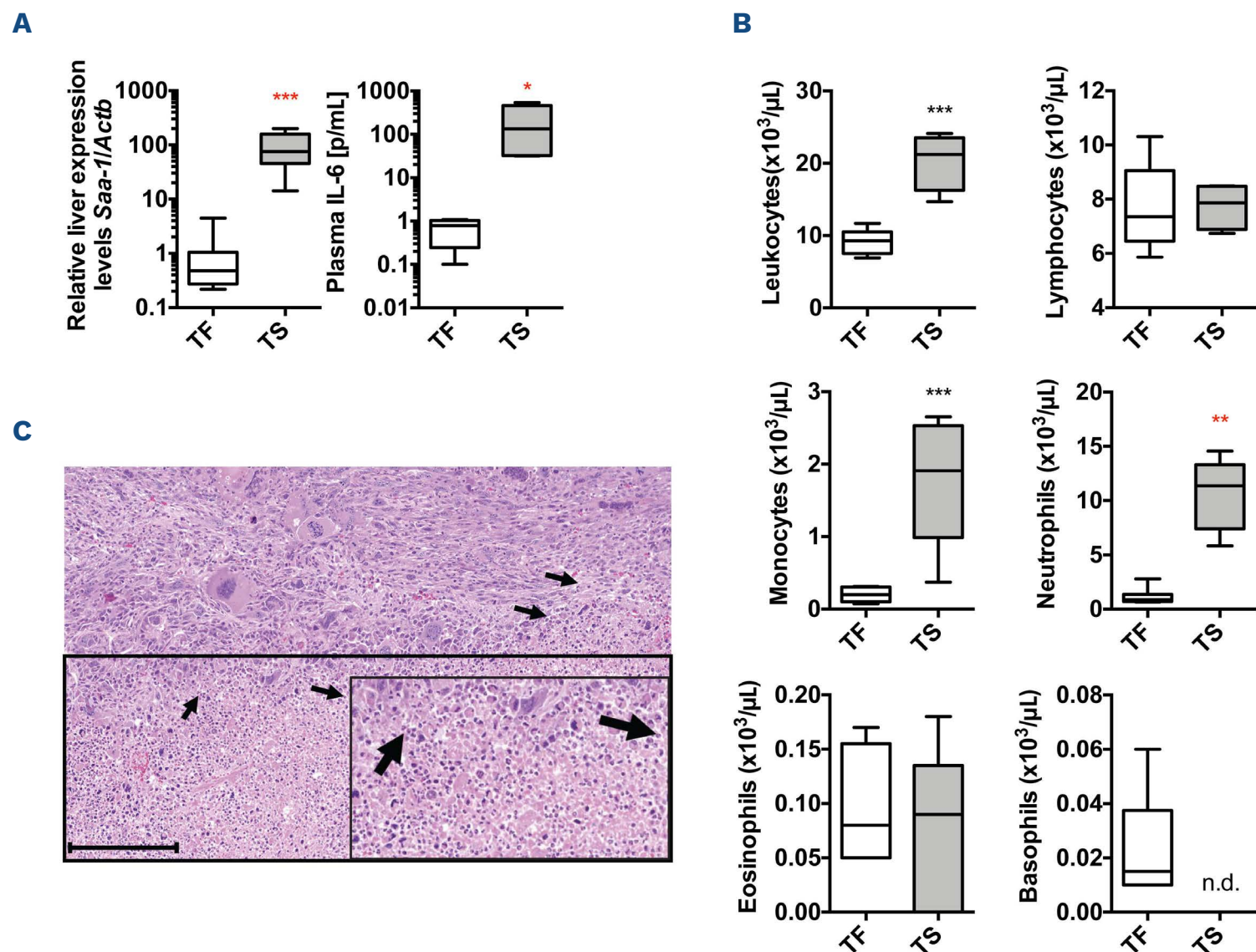


Figure 2. Inflammation in anemic *Trp53^{fllox}WapCre* breast cancer mice. Blood and liver tissue from tumor-bearing *Trp53^{fllox}WapCre* mice (gray boxes) were taken when the tumor reached maximal permitted size (defined as terminal stage, TS). Age-matched tumor-free *Trp53^{fllox}WapCre* mice (TF, white boxes) served as controls. (A) Liver mRNA levels of serum amyloid A 1 (*Saa-1*) (n=14-15) determined by quantitative polymerase chain reaction analysis and normalized to β -actin (*Actb*) mRNA levels (left panel) as well as plasma interleukin-6 (IL-6) levels (n=4), determined by enzyme-linked immunosorbent assay (right panel). (B) Cell counts of leukocytes, lymphocytes, monocytes, neutrophils, eosinophil, and basophils in blood from TF (white boxes) and TS (grey boxes) *Trp53^{fllox}WapCre* mice, analyzed by a Sysmex XT-2000iV. (n.d. not detected) (C) Representative image of suppuratively inflamed tumor regions with massive neutrophil invasion (black arrows representative examples). Scale bar 250 μm . Data are shown as a box plot with minimum to maximum whiskers and were analyzed by a Student *t*-test (black symbols) or a Mann-Whitney test (red symbols) (* $P < 0.05$, ** $P < 0.01$, *** $P < 0.001$).

Impaired erythropoiesis in bone marrow of *Trp53^{fllox}WapCre* mice

To assess erythropoiesis, we quantified five different erythroid maturation stages from proerythroblast to mature red blood cells of Ter119^+ erythroid progenitors¹⁴ in bone marrow and spleen (Figure 4A, *Online Supplementary Figure S8A*). The bone marrow proportion of total Ter119^+ erythroid progenitors decreased 2 times ($P < 0.05$) in TS mice (Figure 4B, *Online Supplementary Figure S8B*). The relative proportion of the different erythroid maturation stages did not change significantly, although proerythroblasts showed an increasing trend ($P = 0.06$) (Figure 4C, *Online Supplementary Figure S8B*). In contrast, the proportion of total Ter119^+ cells in spleens of TS mice did not change but the relative proportion of the erythroid maturation stages increased from 0.8% to 3.2% in proerythroblasts, from 4.7% to 11.7% in basophilic erythroblasts, from 16.0% to 27.2% in polychromatic erythroblasts, and from 6.0% to 14.9% in ortho-

chromatic erythroblasts but decreased from 72.5% to 43.0% in mature red blood cells ($P < 0.05$) (Figure 4C, *Online Supplementary Figure S8B*). In parallel mRNA levels of *Tfrc*, *Trf2*, and *Dmt1* as well as of the erythroid progenitor genes *Epor*, *Gypa*, *Hba*, and *Hbb* increased in the spleens of TS mice, while their expression in bone marrow was reduced (*Online Supplementary Figure S8C*). To test whether erythropoiesis can be boosted by acute iron supplementation during advanced tumor progression, we injected iron into mice harboring tumors larger than 1.5 cm^3 and quantified bone marrow and spleen Ter119^+ erythroid precursors 48 h later. While the Ter119^+ bone marrow proportion of iron-treated tumor mice was 2 times lower ($P < 0.05$) than in iron-treated TF mice, the Ter119^+ spleen proportion increased from 41.6% ($P < 0.05$) in TF to 53.8% ($P < 0.05$) in tumor mice after iron treatment (Figure 4D). Thus, spleen but not bone marrow erythropoiesis profited from iron supplementation, implying that splenic stress erythropoie-

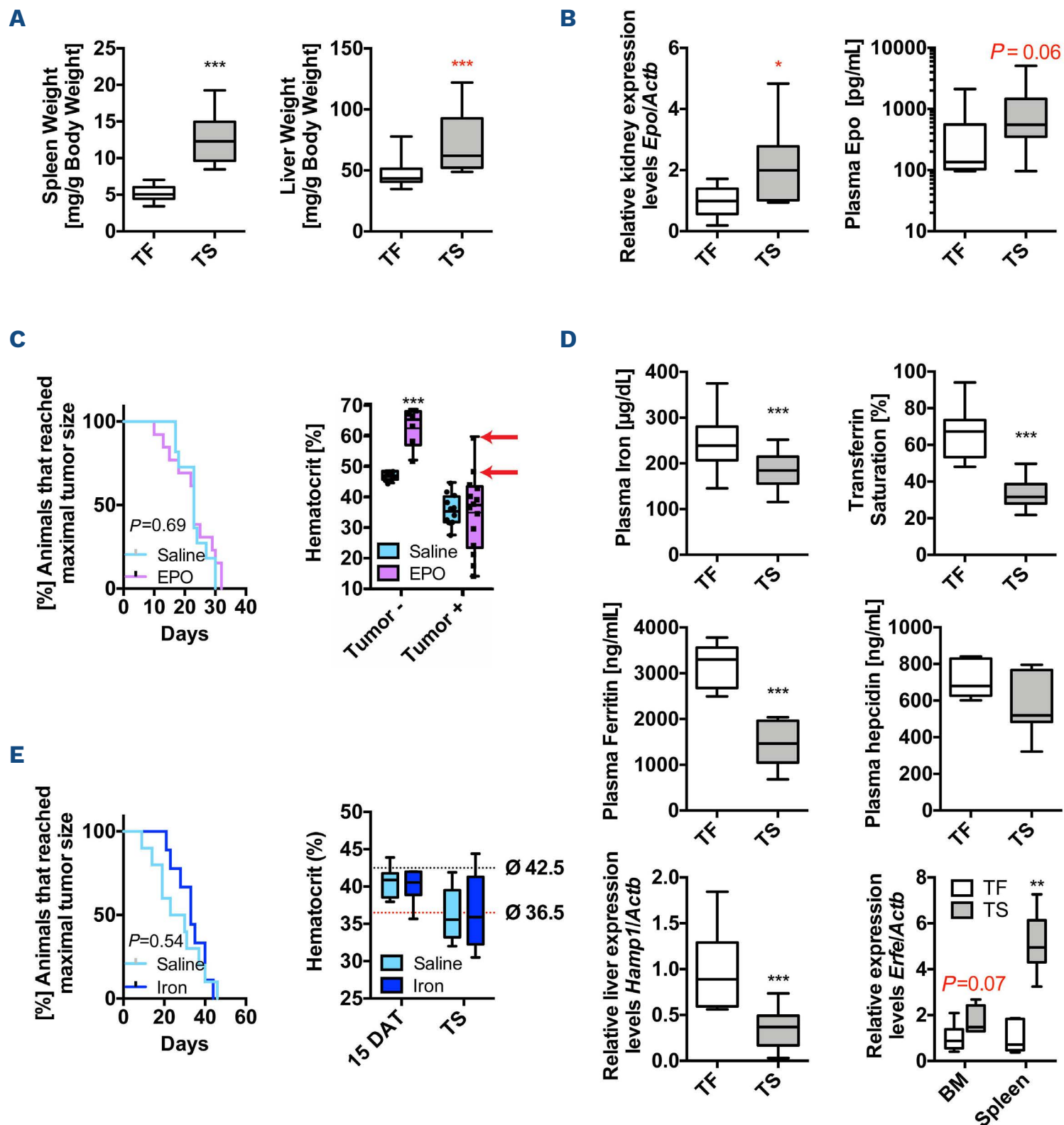


Figure 3. Iron and erythropoietin resistance in hypoferremic *Trp53^{fl}WapCre* breast cancer mice with anemia of cancer. (A, B and D) Tissue and blood from tumor-bearing *Trp53^{fl}WapCre* mice (gray boxes) were taken when the tumor reached maximal permitted size (defined as terminal stage; TS). Age-matched tumor-free *Trp53^{fl}WapCre* mice (TF, white boxes) served as controls. (A) Wet weight of spleen (left panel) and liver (right panel) normalized to the bodyweight. (B) Polymerase chain reaction (qPCR)-quantified erythropoietin (*Epo*) mRNA levels in the kidney normalized to β -actin (*Actb*) (n=9-10) (left panel) as well as EPO plasma levels determined by enzyme-linked immunosorbent assay (ELISA) (n=9-12) (right panel). (C) Immediately after tumor onset, *Trp53^{fl}WapCre* mice were subcutaneously injected with either 1000 U/kg EPO (purple) or saline (light blue) thrice a week until tumors reached maximal size. The modified Kaplan-Meier curve shows the percentage of mice treated with saline (light blue) or 1000 U/kg EPO (purple) which reached maximal tumor size (n=11-13) (left panel). Hematocrit levels of saline-treated (light blue) or 1000 U/kg EPO-treated (purple) tumor mice (Tumor +) as well as TF controls (Tumor -) are also shown (n=6-14) (right panel). Red arrows indicate two EPO-treated mice that showed increased hematocrit values. (D) Plasma iron and transferrin saturation (n=19-20) analyzed by a bathophenanthroline assay (upper panels). Plasma ferritin (n=6) and plasma hepcidin levels (n=5-7) analyzed by ELISA (middle panels). Liver mRNA levels of hepcidin (*Hamp1*) (n=9-11) as well as erythroferrone (*Erfe*) (n=4-6) in bone marrow (BM) and spleen were determined by qPCR and normalized to β -actin (*Actb*) (lower panels). (E) *Trp53^{fl}WapCre* mice were intravenously injected with a single dose of iron (dark blue boxes) or saline (light blue boxes) immediately after tumor onset. In experiment 1, mice received 20 mg/kg Ferinject® and blood as well as tissues were collected 15 days after treatment (15 DAT). In experiment 2, mice received 13.28 mg/kg Ferinject® or saline and blood as well as tissues were collected when the tumor reached maximal permitted size (TS). The modified Kaplan-Meier curve shows the percentage of saline-treated (light blue) and iron-treated (dark blue) mice, which reached maximal tumor size (n=9-10) (left panel) as well as hematocrit (n=8-10) (right panel). The black and red dotted lines in (E) indicate the average values of untreated TF (black dotted line) and untreated TS (red dotted line) mice. Data are shown as a box plot with minimum to maximum whiskers and were analyzed by a Student *t*-test (black symbols) or a Mann-Whitney test (red symbols) (* $P<0.05$, ** $P<0.01$, *** $P<0.001$). Modified Kaplan-Meier curves were analyzed with a log-rank (Mantel-Cox) test.

sis was induced to compensate for the impaired bone marrow erythropoiesis.

Impaired hematopoiesis in bone marrow of $Trp53^{flx}WapCre$ mice

While bone marrow erythroid precursors decreased, the bone marrow cellular density did not differ between TF and TS mice (*Online Supplementary Figure S9A*) indicating that

other cells filled the bone marrow compartment. Indeed, myeloid precursors and mature myeloid cells were enriched in bone marrow smears of TS mice (*Online Supplementary Figure S9B*). To assess hematopoiesis, we analyzed hematopoietic cells by flow cytometry.³⁰ Our data show that neither $CD48^-/CD150^+$ hematopoietic stem cells (HSC) nor $CD48^+/CD150^-$ multipotent progenitors (MMP) differed between TF and TS mice. However, while the bipotent

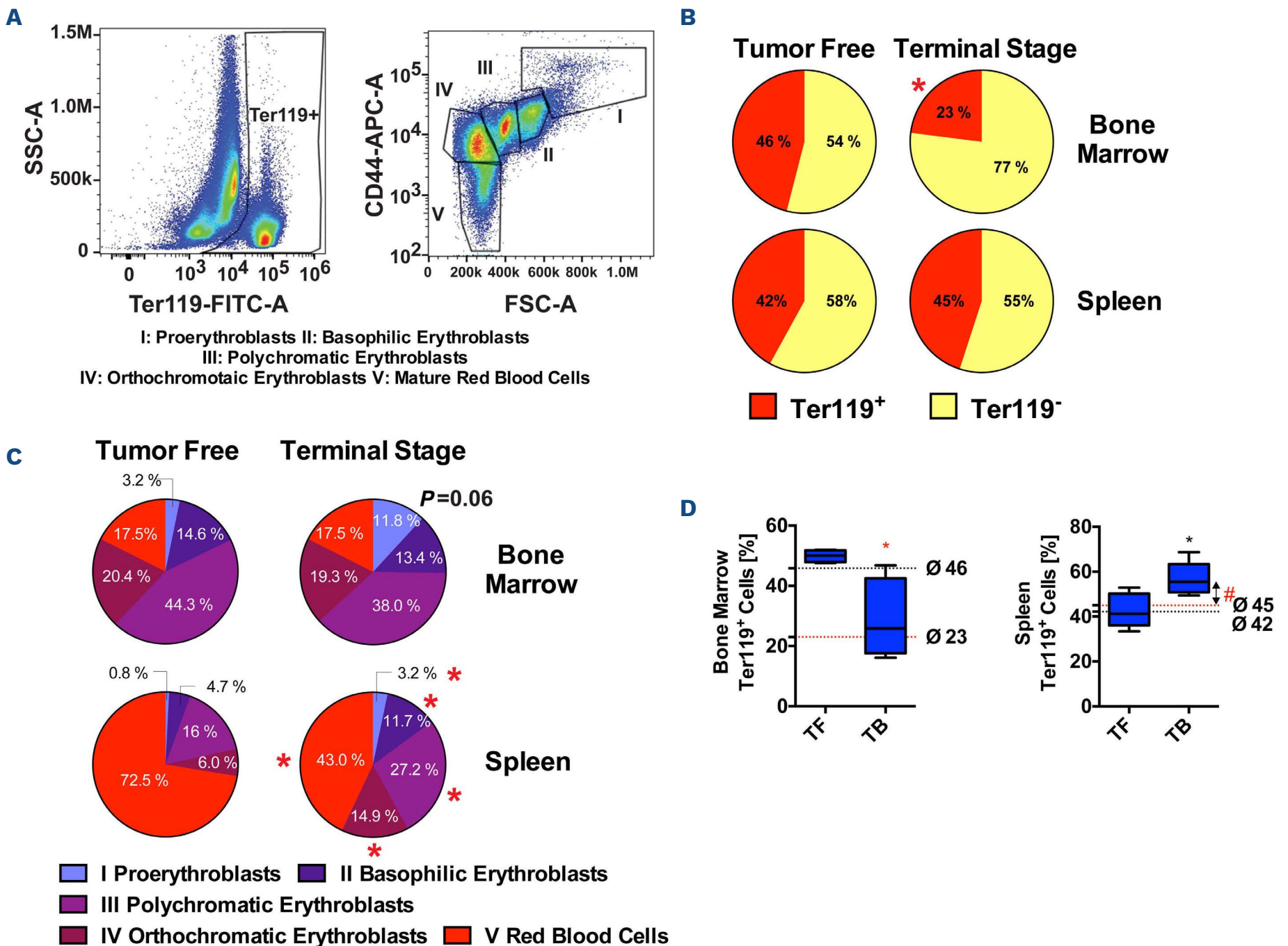


Figure 4. Late-stage erythropoiesis in anemic $Trp53^{flx}WapCre$ mice. Bone marrow and spleen cells from age-matched tumor free (TF) and terminal stage (TS) $Trp53^{flx}WapCre$ mice were collected when the tumors reached maximal permitted size and analyzed by flow cytometry. (A) Representative image of $Ter119^+$ cells (late erythroid precursors) gating in $Ter119^+$ vs. SSC-Area plots (left panel). Different clusters of $Ter119^+$ cells in an FSC-Area vs. CD44 plot (right panel) identified erythroid maturation stages (I: proerythroblasts; II: basophilic erythroblasts; III: polychromatic erythroblasts; IV: orthochromataic erythroblasts (including reticulocytes); and V: mature erythrocytes) based on cell size and CD44 expression levels. (B) Average proportions of $Ter119^+$ (red) and $Ter119^-$ (yellow) cells in bone marrow (upper panels) and spleen (lower panels) from TF (left) and TS (right) $Trp53^{flx}WapCre$ mice analyzed by flow cytometry (n=4). (C) Average proportion of the five maturation stages of erythrocytes (I to V) identified by flow cytometry in an FSC-Area vs. CD44 plot in bone marrow (upper panels) and spleen (lower panels) from TF (left) and TS (right) $Trp53^{flx}WapCre$ mice analyzed by flow cytometry (n=4). (D) Age-matched TF and tumor-bearing (TB) mice received a single intravenous 20 mg/kg iron injection when tumors reached a size of 1.5 cm³. Bone marrow and spleen were harvested 48 h after injection and analyzed by flow cytometry. The proportions of bone marrow (left panel) and spleen $Ter119^+$ cells (right panel) in iron-treated mice (n=4) are shown. Data in (B and C) are shown as average values in pie charts (n=4), data in (D) are shown as a box plot with minimum to maximum whiskers. Data were analyzed by a Student *t*-test (black symbols) or a Mann-Whitney test (red symbols, *P*-values) (****P*<0.001; ***P*<0.01; **P*<0.05). The black and red dotted lines in panel (D) indicate the average values of untreated TF (black dotted line) and untreated TS (red dotted line) mice. #in panel (D) indicates a difference (*P*<0.05) between iron-treated TS and untreated TS (red dotted line) mice.

CD105⁻/CD150⁺ pre-megakaryocyte-erythrocyte progenitors (Pre-MgE) decreased from 0.25% in TF to 0.16% in TS mice ($P=0.06$), the CD105⁻/CD150⁻ pre-granulocyte-monocyte lineage cells (Pre-GM) increased from 0.8% in TF to 1.3% in TS mice ($P<0.05$) (Figure 5A). This suggests that the differentiation of common myeloid progenitors (CMP) was shifted from the erythroid lineage towards the granulo-

cyte-monocyte lineage (Figure 5B). This was further supported by an elevated proportion of CD45⁺/GR1⁺ neutrophil progenitors in bone marrow which increased from 72.5% in TF to 86.5% in TS mice ($P<0.05$). Although the proportion of Pre-MgE was reduced in TS mice, we observed no difference in the proportion of CD150⁺/CD41⁺ megakaryocyte progenitors or CD105⁺/CD150⁺ pre-colony-forming units

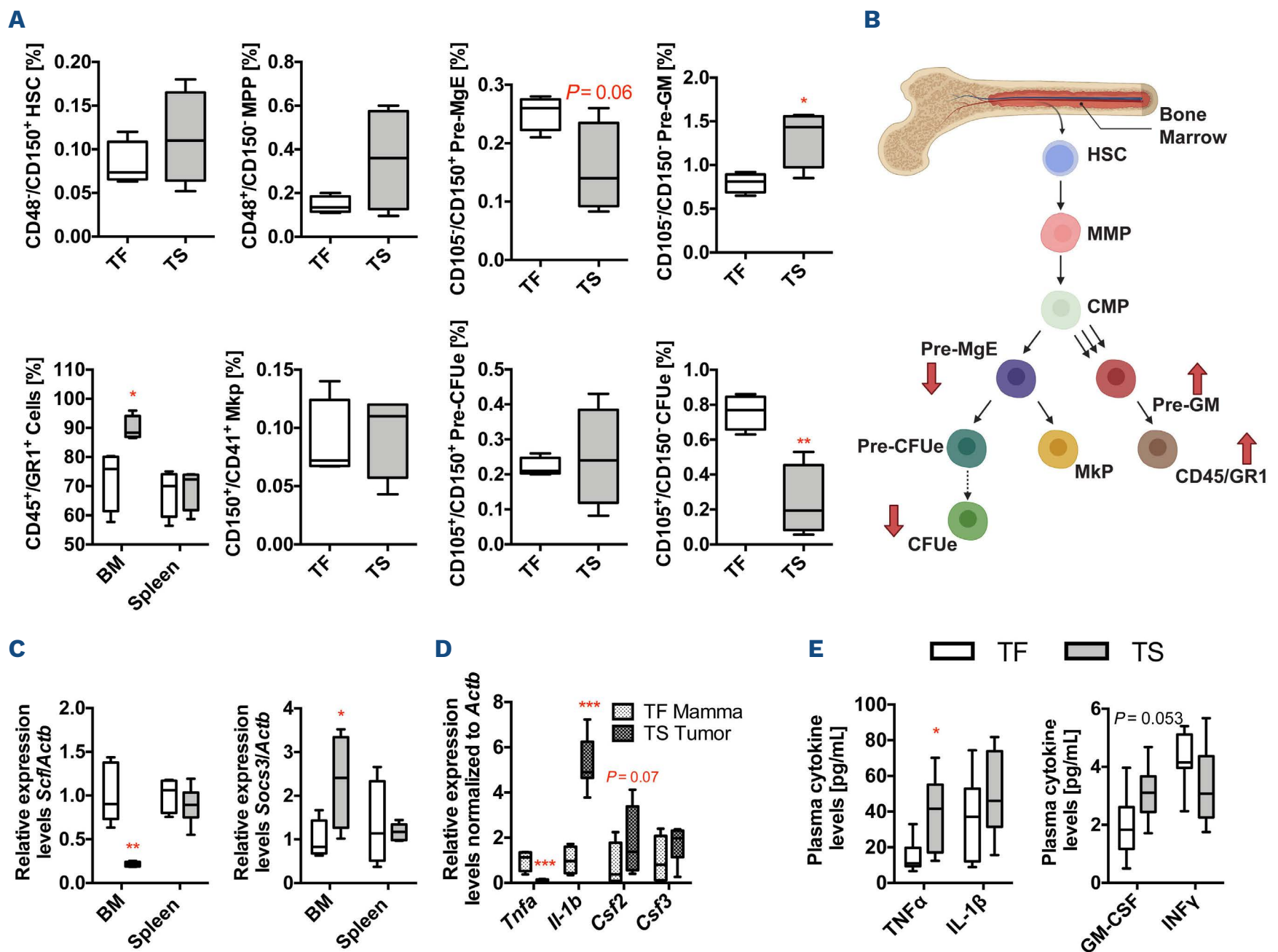


Figure 5. Early-stage hematopoiesis in anemic *Trp53^{fllox}WapCre* mice. (A) Bone marrow and spleen from age-matched tumor free (TF, white boxes) and terminal stage (TS, gray boxes) *Trp53^{fllox}WapCre* mice were collected when the tumors reached maximal permitted size and analyzed by flow cytometry. Proportions of CD48⁻/CD150⁺ hematopoietic stem cells (HSC), CD48⁺/CD150⁻ multipotent progenitors (MPP), CD105⁻/CD150⁺ pre-megakaryocyte erythrocyte progenitors (Pre-MgE), CD105⁻/CD150⁻ pre-granulocyte-monocyte lineage cells (Pre-GM) ($n=4$) are shown. The proportions of CD45⁺/GR1⁺ positive leukocyte precursors in bone marrow and spleen are also shown, as well as CD150⁺/CD41⁺ megakaryocyte precursors (Mkp), CD105⁺/CD150⁺ pre-colony-forming units erythrocyte (Pre-CFUe), and CD105⁺/CD150⁻ colony-forming units erythrocyte (CFUe) in bone marrow ($n=4$). (B) Schematic illustration of the steps of hematopoiesis. The red arrows indicate an up- or down regulation of hematopoietic precursors and the triple black arrows indicate a shift in the maturation of common myeloid progenitors (CMP) towards Pre-GM in the bone marrow of TS *Trp53^{fllox}WapCre* mice. (C) mRNA levels of stem cell factor (*Scf*) (left panel) and suppressor of cytokine signaling 3 (*Socs3*) (right panel) in the bone marrow (BM) and spleen, determined by quantitative polymerase chain reaction (qPCR) and normalized to β -actin (*Actb*) mRNA levels ($n=4-6$). (D) mRNA levels of tumor necrosis factor alpha (*Tnfa*), interleukin 1 beta (*Il-1b*), granulocyte-macrophage colony-stimulating factor (*Csf2*) and granulocyte colony-stimulating factor (*Csf3*) in mammary tissue of tumor free (TF Mamma) and in tumor tissue of terminal stage *Trp53^{fllox}WapCre* mice (TS Tumor), determined by qPCR and normalized to β -actin (*Actb*) mRNA levels ($n=4-8$). (E) Plasma levels of tumor necrosis factor alpha (TNF α) and Interleukin 1 beta (IL-1 β) (left panel) as well as granulocyte-macrophage colony-stimulating factor (GM-CSF) and interferon gamma (INF γ) (right panel) quantified by enzyme-linked immunosorbent assay ($n=7-8$). Data are shown as a box plot with minimum to maximum whiskers and were analyzed by a Student t -test (black P values, panel E) or a Mann-Whitney test (red symbols, P values) (*** $P<0.001$; ** $P<0.01$; * $P<0.05$).

erythrocyte (pre-CFUe) between TF and TS mice. However, the CD105⁺/CD150⁻ colony-forming units erythrocyte (CFUe) decreased from 0.76% in TF mice to 0.24% in TS mice ($P < 0.01$) (Figure 5A). To investigate why erythropoiesis was inhibited in bone marrow but not spleen we analyzed gene expression levels of stem cell factor (*Scf*), which stimulates erythropoiesis,³¹ and suppressor of cytokine signaling (*Socs3*), which inhibits erythropoiesis.²² While *Scf* mRNA levels in bone marrow of TS mice were 4.5 times lower ($P < 0.01$) and *Socs3* mRNA levels 2.3 times higher ($P < 0.05$) than in TF mice, their mRNA levels in the spleen did not differ between TF and TS mice (Figure 5C). Additionally, autophagy genes, which play a critical role in cell organelle removal during erythroid maturation,³² were downregulated in the bone marrow of TS mice (*Online Supplementary Figure S9C*). We also analyzed cytokine mRNA levels in tumors of TS and in healthy mammary tissue of TF mice. Tumor necrosis factor alpha (*Tnfa*) mRNA levels were 9.2 times lower ($P < 0.001$), interleukin 1 beta (*Il1b*) levels were 5.3 times higher ($P < 0.001$), and granulocyte-macrophage colony-stimulating factor (*Csf2*) levels were 2.4 times higher ($P = 0.07$) in tumor tissue, while granulocyte colony-stimulating factor (*Csf3*) levels did not differ between tumor tissue and mammary tissue (Figure 5D). However, the plasma cytokine levels of TNF α increased from 14.6 pg/mL in TF to 40.0 pg/mL in TS mice ($P < 0.05$), the plasma IL-1 β levels did not differ between TF and TS mice and the plasma levels of the myelocytic differentiation regulator GM-CSF increased from 2.0 pg/mL in TF mice to 3.1 pg/mL in TS mice ($P = 0.053$). Additionally measured interferon gamma (INF γ) plasma levels did not differ between TF and TS mice (Figure 5E). Our data suggest that while erythropoiesis may be actively suppressed (e.g., by TNF α), myelocytic differentiation regulators (e.g., GM-CSF) alter the fate of early hematopoietic precursors and prevent erythropoiesis by upregulating myelopoiesis.

Discussion

We examined if Trp53^{fllox}WapCre mice that spontaneously develop breast cancer mirror the human AoC pathology. TS Trp53^{fllox}WapCre mice developed hypochromic AoC together with a strong inflammation and iron deficiency. However, hepcidin levels were not induced and iron deficiency coincided with AoC rather than caused it. Treatment with iron as well as with EPO did not restore normal hemoglobin levels. During early hematopoiesis, the progenitor fate of CMP shifted from erythroid towards the myeloid lineage, resulting in inadequate bone marrow production of red blood cells and excessive production of granulocytes and neutrophils. Pro-inflammatory cytokines such as TNF α and GM-CSF as well as IL-6 may block erythropoiesis and stimulate myelopoiesis independently of hepcidin and iron levels.

Trp53^{fllox}WapCre mice developed AoC associated with an increased number of monocytes and neutrophils in blood, which accumulated in suppuratively inflamed tumor regions. Anemic mice showed slightly upregulated renal *Epo* mRNA as well as EPO plasma levels, probably in response to reduced blood oxygenation. Surprisingly, EPO treatment did not increase hematocrit and hemoglobin levels in TS mice. Non-responsiveness to ESA is also observed in up to 30-40% of human cancer patients³³ either due to inhibited EPO signaling or due to reduced iron availability for erythropoiesis caused by pro-inflammatory cytokines. Especially, IL-6 upregulates hepcidin in the liver, causing functional iron deficiency^{14,15} or it directly inhibits erythropoiesis in patients or mice.^{20,21,34} In anemic Trp53^{fllox}WapCre mice, IL-6 showed by far the highest upregulation of all cytokines assayed. However, while plasma iron levels were reduced, plasma hepcidin levels did not differ between TF and TS mice, and hepcidin mRNA levels in the liver were even reduced. We explain this discrepancy by the enlarged liver in TS mice with more hepcidin-producing cells that compensate the reduced cellular hepcidin synthesis rate. While hepcidin-inducing PDGF-BB²⁹ may not play a major role in our model, the reduced expression of BMP6^{6,7} and the low iron levels *per se*³⁵⁻³⁷ may overwrite the hepcidin-inducing effect of IL-6 that is known from anemia of inflammation.³ Moreover, the increased bone marrow and spleen mRNA levels of *Erfe*⁸ and the increased renal *Epo* mRNA levels suggest that hepcidin may have also been suppressed by the HIF2-EPO-ERFE axis.^{38,39} Hepcidin downregulation in other murine models of AoC was suggested to be a consequence of activated erythropoiesis at late tumor stages, while at early stages, hepcidin expression may be increased by inflammation.¹⁶ In our study, no increase of hepcidin mRNA levels at early or late stages of tumor progression was observed. Furthermore, feeding mice with an iron-sufficient diet (50 mg/kg iron), to exclude the possibility that high iron levels in commercial diets blunt acute hepcidin expression,³ did not alter either hepcidin expression or anemia in our model. We conclude that hepcidin is not the main driver for AoC in Trp53^{fllox}WapCre mice. However, we cannot exclude that inappropriately high hepcidin plasma levels (i.e., no decrease in response to iron deficiency) may contribute to the development of AoC in Trp53^{fllox}WapCre mice. When supplementing tumor mice with iron, hematocrit and hemoglobin values did not increase, although the iron plasma levels were elevated at least until 15 days after treatment. The majority of mice did not fully establish an anemic phenotype during the first 15 days of tumorigenesis and iron supplementation may not have had the desired effect at such early stages. We cannot exclude that higher iron dosages could have protected Trp53^{fllox}WapCre mice better from anemia, despite calculating iron supplementation so that normal hemoglobin values should have been

restored (Ganzoni formula⁴⁰). Moreover, iron supplementation may also increase tumor proliferation⁴¹ but the calculated iron dosages did not cause tumor progression. When mice with advanced 1.5 cm³ large tumors were treated with iron, they had an acute increase in Ter119⁺ erythroid progenitors in the spleen but not in the bone marrow. This suggested that red blood cell production was maintained by the spleen, while it was blocked in the bone marrow where hypoferrremia was not a limiting factor for erythropoiesis and, thus, coincided with AoC in our model.

At late-stage erythropoiesis, the proportion of Ter119⁺ erythroid precursors was reduced in the bone marrow of Trp53^{flox}WapCre mice, while the composition of the erythroid maturation stages from pro-erythroblasts to red blood cells (stage I-V)²⁷ were not significantly altered. In contrast, the proportion of erythroid precursors in the spleens of TF and TS mice did not differ, while the proportion of stages I-IV (pro-erythroblasts to orthochromatic erythroblasts) were increased, and the proportion of the red blood cells (stage V) decreased. We interpret these results in the spleen and the associated splenomegaly as a consequence of stress erythropoiesis and the active release of red blood cells. Similar observations have been made in spleens of mice with abscess-induced inflammation. It was suggested that the accumulation of the maturation stages I-IV results from a blockade of erythroid maturation stage V.⁴²

Neither EPO nor iron treatment prevented AoC in Trp53^{flox}WapCre mice. Therefore, our data suggest that bone marrow erythropoiesis was inhibited prior to iron-dependent maturation stages (erythroblast – reticulocyte) as well as prior to EPO-dependent maturation stages (CFUe – pro-erythroblast). At early hematopoiesis, bone marrow HSC, MPP and CMP did not differ between TF and TS mice. While HSC may be recruited from bone marrow to the spleen resulting in a bone marrow depletion of HSC during AoC,²⁶ the stem cell niche in our model did not appear to be affected. Instead, the commitment of CMP into either Pre-MgE or Pre-GM was shifted in mice. While the proportion of Pre-MgE, including downstream CFUe that give rise to the erythroid lineage, was reduced, the proportion of the myeloid precursors Pre-GM, which give rise to granulocytes,⁴³ was increased, explaining the excessive neutrophil production in Trp53^{flox}WapCre mice. Increased granulocytosis is also observed in human (breast⁴⁴) cancer patients,⁴⁵ in whom it associates with poor survival, as well as in transplanted tumor mouse models.^{46,47} Especially tumor-produced colony-stimulating factors, G-CSF and GM-CSF,^{25,26} which block erythropoiesis by depleting erythroblastic island macrophages⁴⁸ and increasing the number of granulocytes, can cause excessive myelopoiesis.²⁵ Some tumors in cancer patients express G-CSF and GM-CSF associated with an increased number, survival, and activation of neutrophils.^{49,50} While the mRNA levels of both factors in tumors of Trp53^{flox}-

WapCre mice were hardly higher than in healthy mammary tissue, plasma protein levels of myelopoiesis-stimulating GM-CSF were increased, probably contributing to excessive granulocytosis. Increased TNF α levels in Trp53^{flox}WapCre mice suggest that, in addition to promoting myelopoiesis, erythropoiesis-suppressing mechanisms were activated.²³ Indeed, Trp53^{flox}WapCre mice showed increased expression of the EPOR signaling inhibitor SOCS3²² in bone marrow but not in spleen. Additionally, we observed a decreased expression of erythropoiesis-stimulating SCF.⁵¹ However, the plasma levels of TNF α as well as GM-CSF increased less than 3 and less than 2 times, respectively, which challenges their significance in dysregulating bone marrow hematopoiesis in anemic Trp53^{flox}WapCre mice. We speculate that a cocktail of several cytokines, potentially including GM-CSF and TNF α , is required to cause iron- and EPO-resistant AoC. It is also possible that AoC in Trp53^{flox}WapCre mice is predominantly caused by IL-6, which directly suppresses erythropoiesis without increasing hepcidin.

Thus, AoC in Trp53^{flox}WapCre mice differs from one of the most common forms of AoC in humans, in whom iron deficiency plays a key role⁵² and increased hepcidin levels may serve as a serological biomarker for absolute or functional iron deficiency.⁵³ Iron deficiency AoC is often associated with either normocytic (75%) or microcytic (21%) anemia.⁵² We observed macrocytic anemia in Trp53^{flox}WapCre mice (corresponding to observations in 4% of human patients⁵²), which may be a consequence of the severe leukocytosis.⁵⁴ Thus, Trp53^{flox}WapCre mice mimic a rare type of AoC in human patients, in whom bone marrow erythropoiesis is irreversibly suppressed while myelopoiesis is induced.

In conclusion, we characterized AoC in breast cancer Trp53^{flox}WapCre mice and show that hypoferrremia does not cause AoC despite high IL-6 plasma levels, which are expected to activate hepcidin mRNA expression. While the IL-6-induced pathways during anemia of inflammation and AoC largely overlap in humans, IL-6 in mice may activate distinct pathways during anemia of inflammation and AoC. In fact, multiple mouse models, including the herein characterized Trp53^{flox}WapCre mice, develop AoC in response to excessive myelopoiesis suggesting that tumor-induced inflammation alters hematopoiesis prior to erythroid maturation. Trp53^{flox}WapCre tumor mice are, to our knowledge, the first mouse model in which AoC with excessive myelopoiesis cannot be prevented by iron or EPO treatment. Thus, this model will be suitable to study mechanisms of and treatment options for EPO-resistant anemia.

Disclosures

No conflicts of interest to disclose.

Contributions

MG, MUM and MT initiated this project and MT developed it further. NFB contributed to designing experiments, per-

formed mouse and wet laboratory experiments, analyzed and interpreted data, provided intellectual input, and helped to write the manuscript. MR prepared tissue samples, supported iron measurements and evaluated tumor sections. MCdS, OM and SA supported tissue iron measurements, iron staining in tissue sections, and immunohistochemical staining of ferroportin. SA performed hepcidin measurements. MAA, HA, NvB, and JA supported animal experiments and molecular analyses. MS quantified bone marrow smears, JMMR performed Ki67 staining, and VS provided intellectual input. RPS and BW analyzed bone marrow hematopoiesis, and BW also contributed to writing the manuscript. MUM and MG provided intellectual input and helped to write the manuscript. MT designed experiments, contributed to animal experiments, analyzed, and interpreted data, and wrote the manuscript.

Acknowledgments

The authors thank Prof. Thomas Rüllicke (University of Veterinary Medicine Vienna, Austria) for kindly providing the *Trp53^{fllox}WapCre* mouse model and the Center for Clinical Studies of the Vetsuisse Faculty for technical

support. MT thanks Dr. Felix Funk and Dr. Susanna Burckhardt for their valuable scientific input and discussion as well as Vifor Pharma for supporting our independent study.

Funding

MT acknowledges the Thoma Foundation and the Marie-Louise von Muralt Foundation for financial support. MG acknowledges the financial support of the Swiss National Science Foundation and the Humanities at the University of Zurich. MUM acknowledges SFB1036, SFB1118 and DFG (FerroOs - FOR5146) for providing research funding. OM is supported by a Junior Research Grant from the European Hematology Association and an Olympia-Morata-Program fellowship provided by the Medical Faculty of the University of Heidelberg.

Data-sharing statement

All data generated or analyzed during this study are included in this published article and its supplementary information files. Large images are stored on servers of the University of Zurich and are available upon request.

References

- Gilreath JA, Stenehjem DD, Rodgers GM. Diagnosis and treatment of cancer-related anemia. *Am J Hematol*. 2014;89(2):203-212.
- Zhang Y, Chen Y, Chen D, et al. Impact of preoperative anemia on relapse and survival in breast cancer patients. *BMC Cancer*. 2014;14:844.
- Nemeth E, Rivera S, Gabayan V, et al. IL-6 mediates hypoferremia of inflammation by inducing the synthesis of the iron regulatory hormone hepcidin. *J Clin Invest*. 2004;113(9):1271-1276.
- Pigeon C, Ilyin G, Courselaud B, et al. A new mouse liver-specific gene, encoding a protein homologous to human antimicrobial peptide hepcidin, is overexpressed during iron overload. *J Biol Chem*. 2001;276(11):7811-7819.
- Rivera S, Nemeth E, Gabayan V, et al. Synthetic hepcidin causes rapid dose-dependent hypoferremia and is concentrated in ferroportin-containing organs. *Blood*. 2005;106(6):2196-2199.
- Andriopoulos B Jr, Corradini E, Xia Y, et al. BMP6 is a key endogenous regulator of hepcidin expression and iron metabolism. *Nat Genet*. 2009;41(4):482-487.
- Kautz L, Meynard D, Monnier A, et al. Iron regulates phosphorylation of Smad1/5/8 and gene expression of Bmp6, Smad7, Id1, and Atoh8 in the mouse liver. *Blood*. 2008;112(4):1503-1509.
- Kautz L, Jung G, Valore EV, et al. Identification of erythroferrone as an erythroid regulator of iron metabolism. *Nat Genet*. 2014;46(7):678-684.
- Muckenthaler MU, Rivella S, Hentze MW, et al. A red carpet for iron metabolism. *Cell*. 2017;168(3):344-361.
- Wang CY, Xu Y, Traeger L, et al. Erythroferrone lowers hepcidin by sequestering BMP2/6 heterodimer from binding to the BMP type I receptor ALK3. *Blood*. 2020;135(6):453-456.
- Gassmann M, Muckenthaler MU. Adaptation of iron requirement to hypoxic conditions at high altitude. *J Appl Physiol* (1985). 2015;119(12):1432-1440.
- Nemeth E, Tuttle MS, Powelson J, et al. Hepcidin regulates cellular iron efflux by binding to ferroportin and inducing its internalization. *Science*. 2004;306(5704):2090-2093.
- Ganz T, Nemeth E. Hepcidin and iron homeostasis. *Biochim Biophys Acta*. 2012;1823(9):1434-1443.
- Cheng Z, Yan M, Lu Y, et al. Expression of serum BMP6 and hepcidin in cancer-related anemia. *Hematology*. 2020;25(1):134-138.
- Maccio A, Madeddu C, Gramignano G, et al. The role of inflammation, iron, and nutritional status in cancer-related anemia: results of a large, prospective, observational study. *Haematologica*. 2015;100(1):124-132.
- Kim A, Rivera S, Shprung D, et al. Mouse models of anemia of cancer. *PLoS One*. 2014;9(3):e93283.
- Mori K, Fujimoto-Ouchi K, Onuma E, et al. Novel models of cancer-related anemia in mice inoculated with IL-6-producing tumor cells. *Biomed Res*. 2009;30(1):47-51.
- Noguchi-Sasaki M, Sasaki Y, Shimonaka Y, et al. Treatment with anti-IL-6 receptor antibody prevented increase in serum hepcidin levels and improved anemia in mice inoculated with IL-6-producing lung carcinoma cells. *BMC Cancer*. 2016;16:270.
- Rizzo JD, Brouwers M, Hurley P, et al. American Society of Clinical Oncology/American Society of Hematology clinical practice guideline update on the use of epoetin and darbepoetin in adult patients with cancer. *J Oncol Pract*. 2010;6(6):317-320.
- Akchurin O, Patino E, Dalal V, et al. Interleukin-6 contributes to the development of anemia in juvenile CKD. *Kidney Int Rep*. 2019;4(3):470-483.
- McCranor BJ, Kim MJ, Cruz NM, et al. Interleukin-6 directly impairs the erythroid development of human TF-1 erythroleukemic cells. *Blood Cells Mol Dis*. 2014;52(2-3):126-133.
- Liu YX, Dong X, Gong F, et al. Promotion of erythropoietic differentiation in hematopoietic stem cells by SOCS3 knock-

- down. *PLoS One*. 2015;10(8):e0135259.
23. Rusten LS, Jacobsen SE. Tumor necrosis factor (TNF)-alpha directly inhibits human erythropoiesis in vitro: role of p55 and p75 TNF receptors. *Blood*. 1995;85(4):989-996.
 24. Libregts SF, Gutierrez L, de Bruin AM, et al. Chronic IFN-gamma production in mice induces anemia by reducing erythrocyte life span and inhibiting erythropoiesis through an IRF-1/PU.1 axis. *Blood*. 2011;118(9):2578-2588.
 25. DuPre SA, Hunter KW Jr. Murine mammary carcinoma 4T1 induces a leukemoid reaction with splenomegaly: association with tumor-derived growth factors. *Exp Mol Pathol*. 2007;82(1):12-24.
 26. Liu M, Jin X, He X, et al. Macrophages support splenic erythropoiesis in 4T1 tumor-bearing mice. *PLoS One*. 2015;10(3):e0121921.
 27. Chen K, Liu J, Heck S, et al. Resolving the distinct stages in erythroid differentiation based on dynamic changes in membrane protein expression during erythropoiesis. *Proc Natl Acad Sci U S A*. 2009;106(41):17413-17418.
 28. Pronk CJ, Rossi DJ, Mansson R, et al. Elucidation of the phenotypic, functional, and molecular topography of a myeloerythroid progenitor cell hierarchy. *Cell Stem Cell*. 2007;1(4):428-442.
 29. Sonnweber T, Nachbaur D, Schroll A, et al. Hypoxia induced downregulation of hepcidin is mediated by platelet derived growth factor BB. *Gut*. 2014;63(12):1951-1959.
 30. Singh RP, Grinenko T, Ramasz B, et al. Hematopoietic stem cells but not multipotent progenitors drive erythropoiesis during chronic erythroid stress in EPO transgenic mice. *Stem Cell Reports*. 2018;10(6):1908-1919.
 31. Broudy VC, Lin NL, Priestley GV, et al. Interaction of stem cell factor and its receptor c-kit mediates lodgment and acute expansion of hematopoietic cells in the murine spleen. *Blood*. 1996;88(1):75-81.
 32. Mortensen M, Ferguson DJ, Edelmann M, et al. Loss of autophagy in erythroid cells leads to defective removal of mitochondria and severe anemia in vivo. *Proc Natl Acad Sci U S A*. 2010;107(2):832-837.
 33. Tonia T, Mettler A, Robert N, et al. Erythropoietin or darbepoetin for patients with cancer. *Cochrane Database Syst Rev*. 2012;12:CD003407.
 34. Langdon JM, Yates SC, Femnou LK, et al. Hepcidin-dependent and hepcidin-independent regulation of erythropoiesis in a mouse model of anemia of chronic inflammation. *Am J Hematol*. 2014;89(5):470-479.
 35. Girelli D, Nemeth E, Swinkels DW. Hepcidin in the diagnosis of iron disorders. *Blood*. 2016;127(23):2809-2813.
 36. Lasocki S, Millot S, Andrieu V, et al. Phlebotomies or erythropoietin injections allow mobilization of iron stores in a mouse model mimicking intensive care anemia. *Crit Care Med*. 2008;36(8):2388-2394.
 37. Theurl I, Aigner E, Theurl M, et al. Regulation of iron homeostasis in anemia of chronic disease and iron deficiency anemia: diagnostic and therapeutic implications. *Blood*. 2009;113(21):5277-5286.
 38. Duarte TL, Talbot NP, Drakesmith H. NRF2 and hypoxia-inducible factors: key players in the redox control of systemic iron homeostasis. *Antioxid Redox Signal*. 2021;35(6):433-452.
 39. Liu Q, Davidoff O, Niss K, et al. Hypoxia-inducible factor regulates hepcidin via erythropoietin-induced erythropoiesis. *J Clin Invest*. 2012;122(12):4635-4644.
 40. Ganzoni AM. [Intravenous iron-dextran: therapeutic and experimental possibilities]. *Schweiz Med Wochenschr*. 1970;100(7):301-303.
 41. Pfeifhofer-Obermair C, Tymoszyk P, Petzer V, et al. Iron in the tumor microenvironment - connecting the dots. *Front Oncol*. 2018;8:549.
 42. Prince OD, Langdon JM, Layman AJ, et al. Late stage erythroid precursor production is impaired in mice with chronic inflammation. *Haematologica*. 2012;97(11):1648-1656.
 43. Akashi K, Traver D, Miyamoto T, et al. A clonogenic common myeloid progenitor that gives rise to all myeloid lineages. *Nature*. 2000;404(6774):193-197.
 44. Tabuchi T, Ubukata H, Saniabadi AR, et al. Granulocyte apheresis as a possible new approach in cancer therapy: a pilot study involving two cases. *Cancer Detect Prev*. 1999;23(5):417-421.
 45. He H, Zhang Z, Ge J, et al. Leukemoid reaction associated with transitional cell carcinoma: a case report and literature review. *Niger J Clin Pract*. 2014;17(3):391-394.
 46. Lan S, Rettura G, Levenson SM, et al. Granulopoiesis associated with the C3HBA tumor in mice. *J Natl Cancer Inst*. 1981;67(5):1135-1138.
 47. Thomas E, Smith DC, Lee MY, et al. Induction of granulocytic hyperplasia, thymic atrophy, and hypercalcemia by a selected subpopulation of a murine mammary adenocarcinoma. *Cancer Res*. 1985;45(11 Pt 2):5840-5844.
 48. Jacobsen RN, Forristal CE, Raggatt LJ, et al. Mobilization with granulocyte colony-stimulating factor blocks medullar erythropoiesis by depleting F4/80(+)VCAM1(+)CD169(+)ER-HR3(+)Ly6G(+) erythroid island macrophages in the mouse. *Exp Hematol*. 2014;42(7):547-561 e4.
 49. Bahar B, Acedil Ayc Iota B, Coskun U, et al. Granulocyte colony stimulating factor (G-CSF) and macrophage colony stimulating factor (M-CSF) as potential tumor markers in non small cell lung cancer diagnosis. *Asian Pac J Cancer Prev*. 2010;11(3):709-712.
 50. Curran CS, Evans MD, Bertics PJ. GM-CSF production by glioblastoma cells has a functional role in eosinophil survival, activation, and growth factor production for enhanced tumor cell proliferation. *J Immunol*. 2011;187(3):1254-1263.
 51. Zsebo KM, Williams DA, Geissler EN, et al. Stem cell factor is encoded at the Sl locus of the mouse and is the ligand for the c-kit tyrosine kinase receptor. *Cell*. 1990;63(1):213-224.
 52. Park S, Jung CW, Kim K, et al. Iron deficient erythropoiesis might play key role in development of anemia in cancer patients. *Oncotarget*. 2015;6(40):42803-42812.
 53. Shu T, Jing C, Lv Z, et al. Hepcidin in tumor-related iron deficiency anemia and tumor-related anemia of chronic disease: pathogenic mechanisms and diagnosis. *Eur J Haematol*. 2015;94(1):67-73.
 54. Small T, Oski FA. The mean corpuscular volume (MCV) in children with acute lymphoblastic leukemia. *Clin Pediatr (Phila)*. 1979;18(11):687-688, 690-691.